# Diabatic modification of air masses along a warm conveyor belt

Oscar Martínez-Alvarado
Robert Plant
John Methven

August 12, 2011

## 1 Introduction

One ambition of the DIAMET flight campaigns is to infer net diabatic heating following a warm conveyor belt (WCB) through the quasi-Lagrangian analysis of flight legs across the WCB separated in time. There are two aspects that make this endeavour difficult:

1. turbulent mixing between air masses, especially potential temperature and humidity
2. variability within air masses and the method of linking two flight segments to infer changes following air masses

This document explores the feasibility of such an analysis by simulating a case using the Unified Model and then sampling the WCB by taking sections across it that move downstream with the air in the WCB. The movement of air and changes in its properties are investigated using trajectories. At this stage we have not explored the more constrained scenario that the sections cannot be made moving downstream with the WCB and instead sections are made across the WCB in roughly the same location relative to the ground but separated in time. This would require a "frozen coherent structure" hypothesis where the WCB is assumed to change structure little over the time interval between the sections and translates with the system velocity.

The case under analysis is the T-NAWDEX III case that took place on 24 November 2009 during the T-NAWDEX pilot campaign. This case was characterised by a system with a strong WCB and has already been subject of study using sources and sinks of potential vorticity. The method of analysis presented here intends to emulate a hypothetical flight with sections across the system's cold front and WCB at a reference time and subsequent passes after 2 hours and 6 hours. The reference time considered here is 0100 UTC 24 November 2009. This time as well as the subsequent passes and the sections considered here are by no means fixed and can be adjusted according with each case's needs.

## 2 Numerical simulation

Figure 1 shows the state of the system at 0100 UTC 24 November 2009 as simulated by the MetUM version 7.3. The simulation started at 0000 UTC 22 November 2009 with initial condition taken

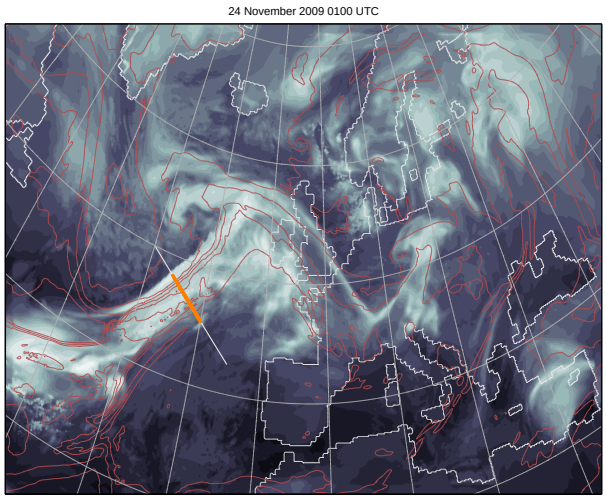


Figure 1: Model-derived OLR and $\theta_e$ on model level 13 (3.38 km, red contours). The white line represents the position of the vertical section in Fig. 2. Orange dots show the horizontal projection of trajectory parcels' initial positions.

from a Met Office global operational analysis. A global simulation was performed to generate lateral boundary conditions for the LAM simulation presented here. This simulation was performed on the standard North Atlantic - Europe domain ($360 \times 600$ gridpoints) and had a horizontal grid spacing of $0.11^\circ$ (approximately equivalent to 12 km) and 38 vertical levels with lid around 39 km).

# 3 Initial distribution of $\theta$ and moisture

Figure 2 shows the distribution of potential temperature $\theta$ (Fig. 2a), cloud liquid content $q_{cl}$ (Fig. 2b) and cloud ice content $q_{cf}$ (Fig. 2c) on the cross-front vertical section (white line) indicated in Fig. 1. The latter two variables provide us with an idea of the vertical structure of the cold front and the WCB. In particular we notice the sharp increase in $\theta_e$ horizontal gradient due to the enhanced presence of water vapour along the cold front. In terms of the vertical distribution of cloud we notice that above the freezing level (0 C) practically all water content is in ice phase rather than a liquid-ice mixture.

# 4 Trajectory analysis

Forward trajectory analysis was used to investigate the redistribution of air within the WCB. Trajectories were initialised as a subset of parcels belonging to the WCB within the vertical section in Fig. 2. In order to select these parcels three criteria have been applied:

1. Initial longitude between 20°W and 26°W.
2. Wind speed in the interval $15 \leq |\mathbf{U}| \leq 60$ m s$^{-1}$
3. Equivalent potential temperature in the interval $295 \leq \theta_e \leq 315$ K

These parcels were coloured by their initial $\theta_e$ value (at 0100 UTC), which is assumed constant throughout the analysis, an assumption that will be proved reasonably accurate later. The initial

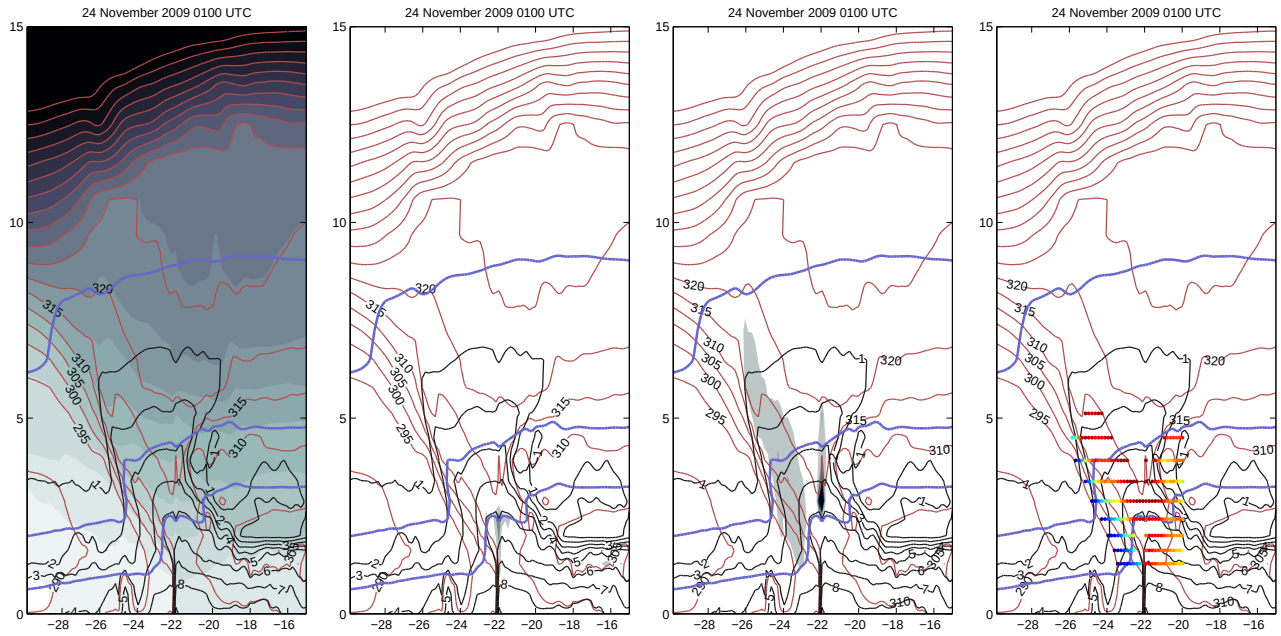


Figure 2: Vertical section through the white line in Fig. 1 showing (a) $\theta$, (b) $q_{cl}$, (c) $q_{cf}$ and (d) initial distribution of WCB parcels coloured by their $\theta_e$ value at the time shown (dark blue representing $\theta_e \leq 295$ and dark red representing $\theta_e \geq 315$). Also shown are $\theta_e$ (red), $q$ (black) and isotherms for 0 C (lower blue), −10 C (middle blue) and −40 C (upper blue).

distribution of WCB parcels is shown in Fig. 2d. The distribution of these parcels is also indicated in Fig. 1 (orange dots). The location of these parcels at 0300 UTC, 0500 UTC and 0900 UTC is shown in Fig. 3. At least two different streams can be appreciated in the latter figure. There is a set of trajectories that move slowly in a relatively cloud-free region within the warm sector to the south of the WCB. To the north, directly within the cloudy region there is a second set of trajectories that move with the cloud. This set of trajectories constitute part of the WCB. A strong wind shear is made evident by the deformation of the original section. It can be shown that parcels at upper levels travel faster as they are steered by the upper level jet. Figure 4 shows the position of the parcels in a 400-km band centred around the sections indicated by white lines in Fig. 4b–c. These parcels are coloured as in Fig. 2d.

## 4.1 Changes in $\theta$ and moisture along trajectories

Figure 5 shows the change in $\theta$, $\theta_e$ and $q$ (or ln $q$) following trajectories between 0100 UTC and 0500 UTC. In unsaturated air we expect that all three variables are conserved in the absence of mixing: therefore any changes result from mixing. A characteristic of mixing between two distinct air masses is that any two conserved variables are linearly related to each other on tracer-tracer scatter plots. In saturated air experiencing condensation but little mixing we would expect $\theta_e$ to be conserved, but $q$ to decrease and $\theta$ to increase from latent heat release. However, typically ascending air masses experience strong mixing associated with shear turbulence and convection and this will affect all three variables. The leading question is whether changes associated with latent heat release can be partitioned from mixing in this scenario.

The air masses show different behaviour depending on their initial value of $\theta_e$. For $\theta_e \geq 305$ K (Fig. 5a) changes in $\theta_e$ are much smaller than those in $\theta$ suggesting that latent heat release is occur-

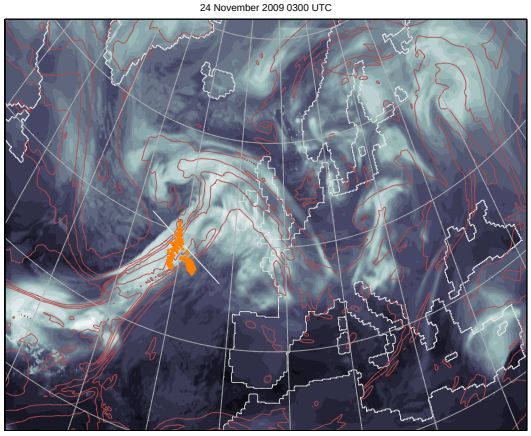


(a)

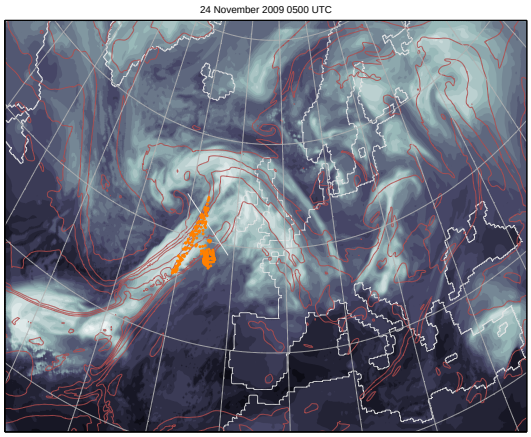


(b)

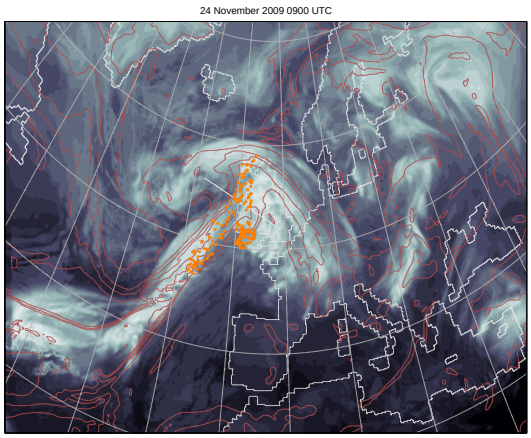


(c)

Figure 3: Model-derived OLR maps showing snapshots of the system's evolution at (a) 0100 UTC, (b) 0300 UTC, (c) 0500 UTC and (d) 0900 UTC on 24 November 2009. Red contours represent $\theta_e$ isolines on model level 13 (3.38 km). Green dots represent the position of a trajectory ensemble starting from the section in Fig. 2. White line segments represent the positions of the vertical sections in Fig. 4.

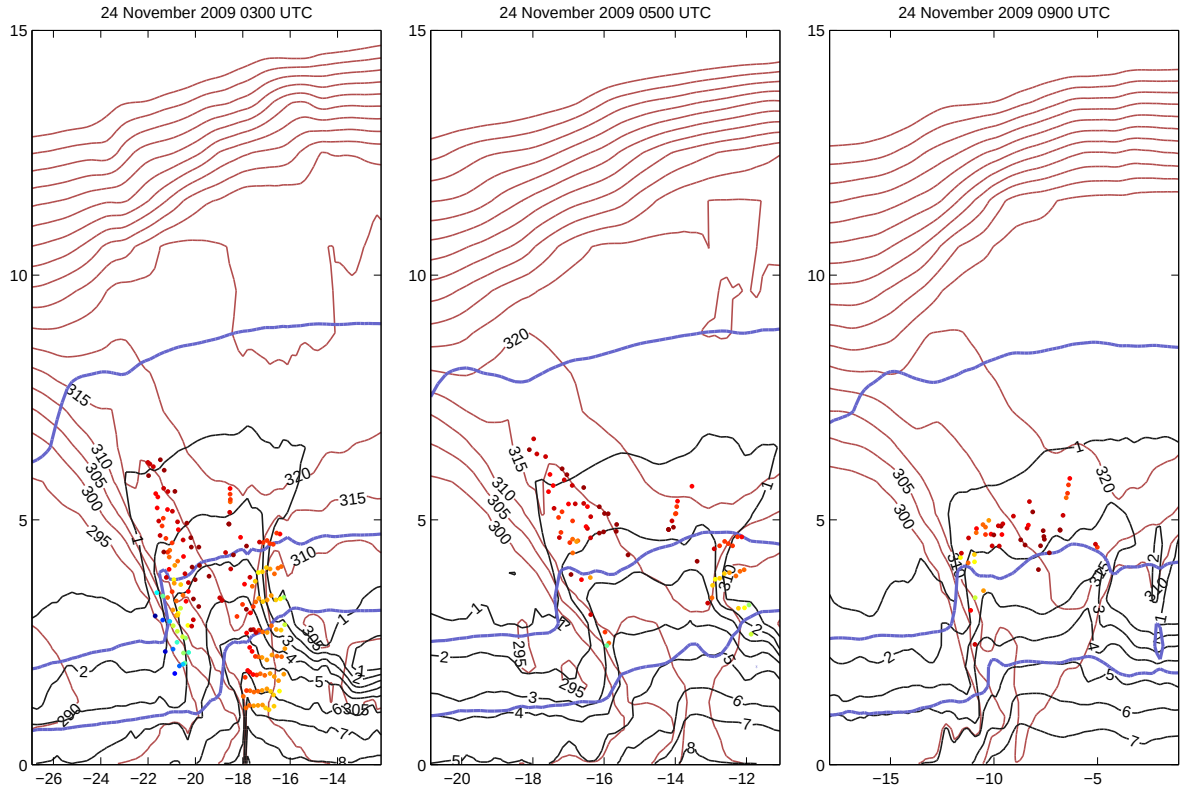


Figure 4: Vertical section corresponding to the white line segments in Fig. 3 showing subsequent positions of a trajectory ensemble starting from the section at 0100 UTC. The parcels have been coloured as in Fig. 2d. Also shown are $\theta_e$ (red), $q$ (black) and isotherms for 0 C (lower blue), $-10$ C (middle blue) and $-40$ C (upper blue).

ring. In addition $\Delta \ln(q)$ decreases roughly linearly with $\Delta\theta$ as might be expected from condensation. However, this does not rule out the possibility that mixing accounts for some of the change and the slope of $\Delta\theta_e$ to $\Delta\theta$ is related to the gradients in the two fields on the west side of the WCB.

For $\theta_e < 305$ K (Fig. 5b) some trajectories experience a large increase in $\theta_e$ which can only be accounted for by mixing. The increase in $\theta$ is similar (the slope is $\sim 1$ on the $\Delta\theta_e$ vs $\Delta\theta$ plot). There is no evidence for latent heat release. There is however a cluster of trajectories that experience a decrease in $\theta$ and increase in $q$ while $\theta_e$ is constant. This is indicative of evaporative cooling.

# 5 Measurability

The previous section used model data sampled along calculated trajectories and showed that changes in air masses properties are likely to be large enough relative to variability to detect if we knew exactly where all trajectories were going and if we could sample them twice. However, we do not know the exact trajectories of air parcels and mixing also makes a Lagrangian link in time non-unique. When the values of $\theta$, $\theta_e$ and moisture are plotted from cross-sections made at two times the task of measuring differences between times seems more challenging.

Figure 6 shows these plots for a time interval of two hours. Once again the parcels have been separated according to their $\theta_e$ initial value. After this short period the regions occupied by the parcels are virtually the same making it impossible to distinguish them.

After six hours (Fig. 7 parcels with $\theta_e \geq 305$ K remain largely in the same region although some

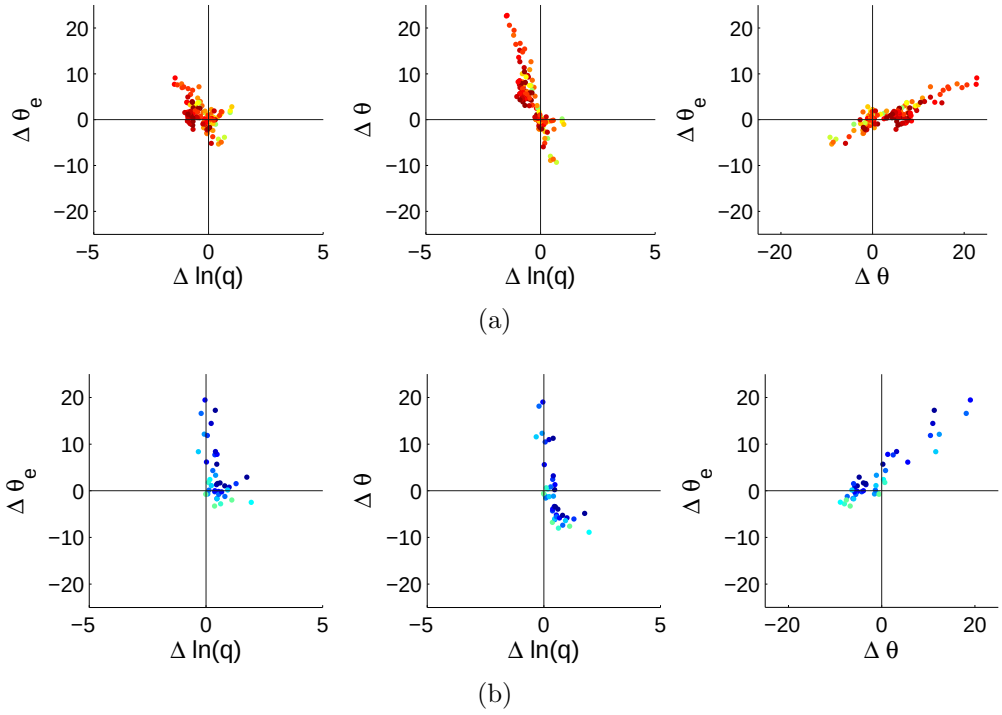


(a)

(b)

Figure 5: Increments in $\theta$, $\theta_e$ and $q$ between 0100 UTC and 0500 UTC for those parcels shown in Fig. 4a. The parcels have been coloured according to their $\theta_e$ value at 0100 UTC. (a) Trajectories with initial $\theta_e \geq 305$ K; (b) Trajectories with initial $\theta_e < 305$ K.

degree of separation is now present for the parcels that contained most moisture initially (Fig. 7a). Parcels with $\theta_e < 305$ K, on the other hand, seem to have separated to a large extent (Fig. 7b). However, this is mainly due to mixing so that $\theta_e$ has also been modified, as previously discussed.

The problem here is clear: there is no way from these observations alone to link the red and blue points in the scatter plots (although they are linked by model trajectories) and the clusters of points have a large degree of overlap. There are a number of ways to attempt to do better: i) more selective use of "observations" upstream and downstream and ii) use of other tracers.

Figure 8 shows the same section as in 2 and the starting location of parcels. The parcels have been coloured by the change in $\theta$ experienced following their trajectories split into two groups: parcels with initial $\theta_e \geq 305$ K (upper row) and $\theta_e < 305$ K (lower row). The first column (Fig. 8a,c) shows the changes after two hours (between 0100 UTC and 0300 UTC). The second column (Fig. 8b,d) shows the changes after six hours (between 0100 UTC and 0700 UTC) This figure confirms that if time interval is too short (two hours) the changes in $\theta$ would be hardly detectable. For the longer interval (six hours) there is an important number of parcels that are not exhibiting a measurable change in $\theta$. This parcels are part of the warm sector rather than the WCB and constitute the first stream of trajectories noted in Sec. 4. The parcels that do belong to the WCB exhibit a larger change in $\theta$ that appears to be detectable and measurable ($\Delta\theta > 5$ K).

This suggests that we should be more selective in isolating air masses for the conserved-variable diagram analysis shown in Fig. 7. Also it is clear that points coinciding with the frontal gradient itself are better ruled out (since $\Delta\theta$ is both negative and positive and likely dominated by mixing).

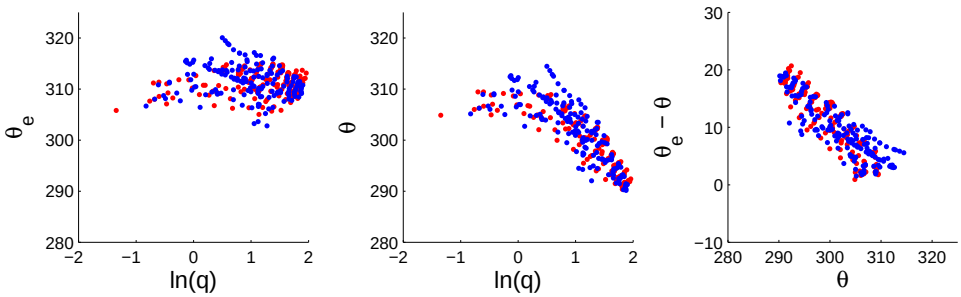


(a)

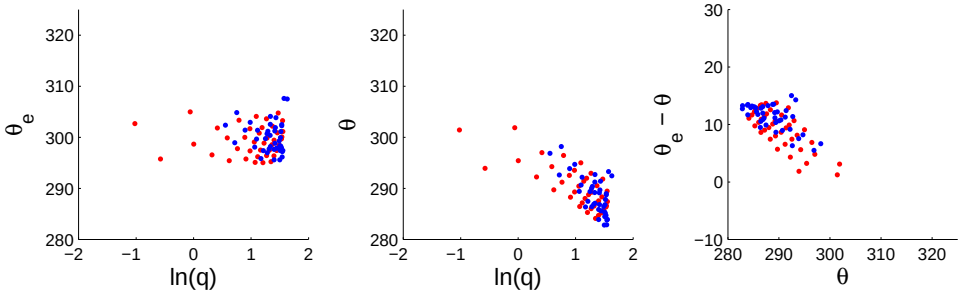


(b)

Figure 6: Scatter plots in the $\theta$-$\theta_e$-ln($q$) at 0100 UTC (red dots) and 0300 UTC (blue dots) for those parcels shown in Fig. 4a. (a) Trajectories with initial $\theta_e \geq 305$ K; (b) Trajectories with initial $\theta_e < 305$ K.

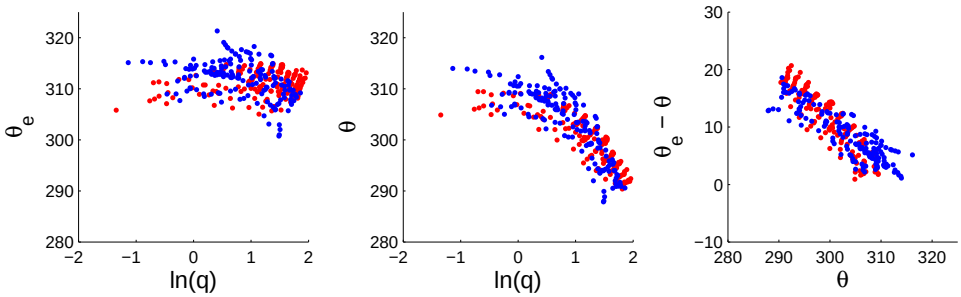


(a)

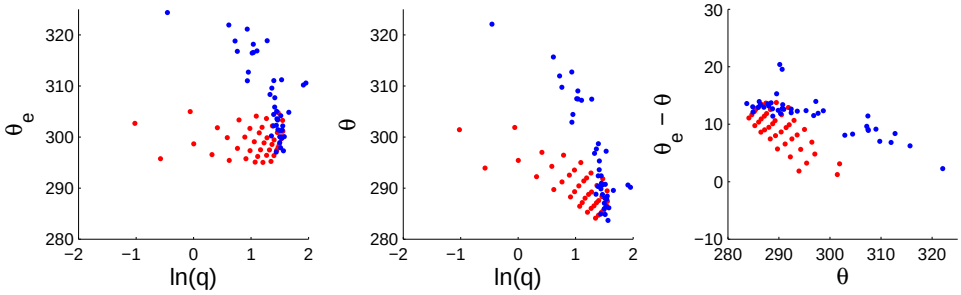


(b)

Figure 7: As in Fig. 6, but for the interval between 0100 UTC (red dots) and 0700 UTC (blue dots).

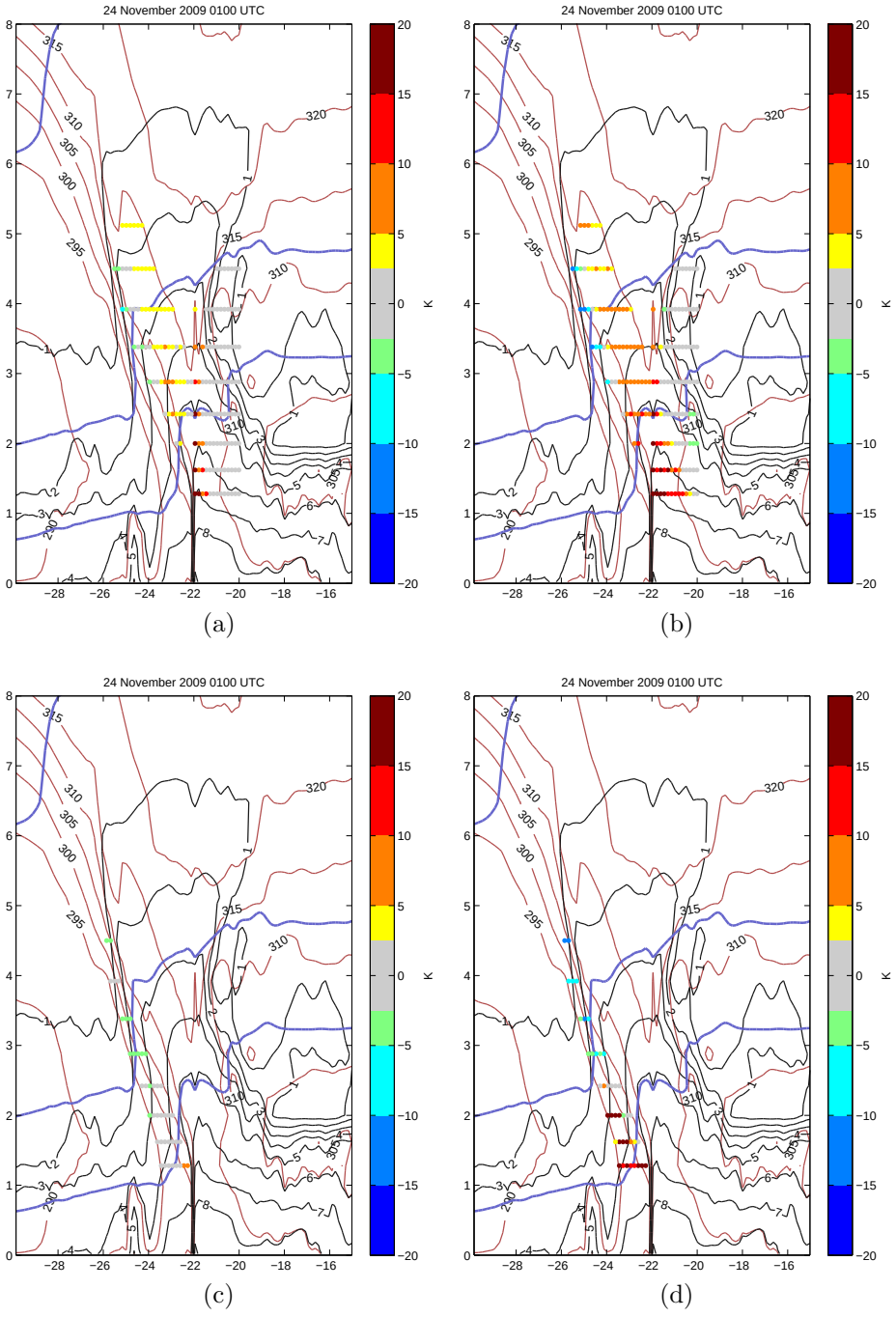


Figure 8: Vertical section through the white line in Fig. 1 showing the initial distribution of WCB parcels coloured by changes in $\theta$ for intervals starting at 0100 UTC and ending at (a,c) 0300 UTC and (b,d) 0700 UTC for (a,b) trajectories with initial $\theta_e \geq 305$ K and (c,d) trajectories with initial $\theta_e < 305$ K. Also shown are $\theta_e$ (red), $q$ (black) and isotherms for 0 C (lower blue), $-10$ C (middle blue) and $-40$ C (upper blue).

# 6 Conclusions

1. The magnitude of changes in $\theta$ following air masses is detectable but the two "Lagrangian sections" need to be separated by greater than 2 hours. This essential rules out the possibility of achieving this kind of analysis with one flight. A six hour separation does appear to be sufficient, which would be possible with a double header flight with a few hours on the ground inbetween. An even longer separation would be desirable, but clearly the air moves a long way in that time and the structure of the WCB also evolves. Both these effects render the Lagrangian matching of data much more difficult.

2. Mixing also renders the analysis difficult. However, if chemical tracers can be used to isolate better Lagrangian links between upwind and downwind sections it looks as though the net change in $\theta$ should be detectable over 6 hours from data alone. Previously it has been possible to estimate photochemical changes in ozone using $\theta_e$ and $q$ as air mass labels, although for much longer time separations in cases where mixing is weak. Here, the aim would be to infer $\Delta\theta$ using ozone and CO as labels. Fortunately, due to cloud the chemical processing within a WCB is much slower than mixing and all the tracers experience the same advection and mixing. At the very least, ozone-CO mixing lines enable us to rule out flight segments on the strongest gradients where the inference of heating would be impossible.

3. Conserved variable diagrams would be better if we incorporated the liquid and ice phases into "total water" mixing ratio and a more sophisticated equivalent potential temperature that includes condensate. Does anyone have experience doing this with the BAe146 data? What is the uncertainty in estimates of ice phase mixing ratio?

4. Since trajectories calculated from analyses are sufficiently accurate to represent mesoscale structure in RDF sections, we could use them to isolate segments of upwind and downwind data that are linked following the analysed flow.

5. The Unified Model will be run for the flight days and so the analysis presented here can be applied and compared with using scatter plots of model and observed data from flight sections. We are looking for deviations of the model from observed behaviour (that is not associated with simple displacement error of the front/WCB).

6. The partition of $\Delta\theta$ by process is difficult. It will largely be reliant on the $q$ and $\theta$ tracers in the Unified Model simulations that accumulate tendencies from the different processes in the model. These tracers have been run for the case shown here and will be the focus of the next stage of work.